Available online at www.sciencedirect.com

ScienceDirect

Procedia Engineering 148 (2016) 18 – 24

Procedia Engineering

www.elsevier.com/locate/procedia

4th International Conference on Process Engineering and Advanced Materials

Activated Carbon Bio-Xerogels as Electrodes for Super Capacitors Applications

Zulamita Zapata-Benabithe[a,*], Giovanna Diossa[a,b], Chris.D. Castro[b], Germán Quintana[b]

[a]*Grupo de Energía y Termodinámica, Facultad de Ingeniería Química, Universidad Pontificia Bolivariana, Circular 1No 70-01, Medellín 050031, Colombia*
[b]*Grupo Pulpa y Papel, Facultad de Ingeniería Química, Universidad Pontificia Bolivariana, Circular 1No 70-01, Medellín 050031, Colombia*

Abstract

The objectives of this work are to evaluate the use of the lignin as precursor of carbon xerogels and to determinate the effect of porosity and surface functionalities on the electrochemical capacitance of the activated carbon bio-xerogels. Lignin replaced the resorcinol at a mass fraction between 0 and 0.086 (wt%). The organic carbon xerogels are H_3PO_4-activated at H_3PO_4/carbon ratio of 1/1 at 450 ºC to increase pore volume and surface area. Gravimetric capacitance values at 0.125 A/g, in a three-cell configuration, ranged from 138 to 234 F/g. Sample with a 0.086 content of lignin showed the best electrochemical behavior, which was associated with the high BET surface area (1243 m^2/g), high volume ($W_0(N_2)$= 0.518 cm^3/g) and width micropores ($L_0(N_2)$= 1.43 nm) and to the presence of pseudo faradic effects.

Peer-review under responsibility of the organizing committee of ICPEAM 2016

Keywords: Lignin; Activated carbon xerogels;Supercapacitors

1. Introduction

Since their synthesis by Pekala [1], carbon gels have been widely studied due to their interesting properties like high surface area, controlled porous structure, low bulk density, electrical conductivity, etc., that make them suitable for several applications such as catalyst support [2,3], insulator [4], electrode for supercapacitors [5,6], fuel cells [3,7], etc. All carbon xerogels properties can be designed by using different precursors, synthesis conditions, drying methods, thermal treatments and/or activation processes. However, the raw materials and long production process are quite expensive so the resulting products are not yet widely commercially available; currently it has been demonstrated that new and cheaper precursors, as lignin, can be used keeping their textural properties; normal convection drying and chemical activation also help to reduce costs [8].

Lignin is the second most abundant biopolymer after cellulose. It is extremely low cost and of phenolic nature. It has been found that lignin is an excellent precursor of activated carbon and bioadsorbent, thanks to its high molecular weight polymer complex structure and the presence of different high electron density functional groups such carboxylic, carbonyl, hydroxyl and ketone [9].

Although several works synthetize carbon gels with lignin, having good textural properties [10–12], there is no further information about their performance on the multiple applications of carbon gels, mainly electrode for supercapacitors. Supercapacitors are a promising technology that could replace batteries in different areas like load levelling and electrical energy

* Corresponding author. Tel.:+0-574-448-8388; fax:+0-574-448-8388.
E-mail address: zulamita.zapata@upb.edu.co

Peer-review under responsibility of the organizing committee of ICPEAM 2016
doi:10.1016/j.proeng.2016.06.470

storage devices; they also could be used in applications that required rapid charge/discharge, high power, etc. [13].

In this work, lignin carbon xerogels were prepared by chemical activation with phosphoric acid. The main objective is to investigate the effect of lignin incorporation on porosity, surface functionalities and their electrochemical capacitance.

2. Experimental Details

2.1. Preparation of activated carbon bio-xerogels

Lignin was supplied by Propal Company (Cali, Colombia) obtained by extraction of black liquor from alkaline pulping process and was obtained according to the methodology showed in [14]. Soda lignin was precipitated from sugar cane bagasse soda pulping black liquor by acidification with sulfuric acid at 98 % until the pH of the resultant solution was close to 2.The precipitate was washed with water until the pH of the rinse was close to 6, dried in an oven at 105 ºC for 24 h, and a dark-brown powder was recovered.

The organic bio-xerogels, CG, were prepared by the sol-gel polymerization reaction of resorcinol (R) and lignin (L) with formaldehyde (F) in water (W) using sodium hydroxide as catalyst (C). Resorcinol was partially replaced for Lignin at different percentages as showed in Table 1. The (R+L)/F, (R+L)/W and (R+L)/C mass ratios were kept constant at 1.86, 0.62 and 90.3, respectively. The mixtures were cured at 85 ºC for 5 days, cut into 5 mm pellets, washed several times with ethanol and dried at atmospheric pressure at 40 ºC up to constant weight of dry gel. Table1 also are presented the pH of initial dissolutions and the bulk density of the dried organic xerogels.

Portions of organics xerogels were ground and sieved between 0.5 and 1 mm and impregnated with a H_3PO_4 aqueous solution to give H_3PO_4/carbon weight ratio of 1/1. The slurries were heated at 450 ºC for 2 h, washed several times with water and finally dried at 120 ºC. The resultant activated carbon xerogels were termed as CG0A, CG22A and CG27A, according to the percentage of lignin added.

Table 1. Mass fractions, mass ratio and pH of initial dissolutions and bulk density dried organic bio-xerogels.

Sample	L (m.f.)	R (m.f.)	W (m.f.)	F (m.f.)	NaOH (m.f.)	L/(L+R)*100 (*wt/wt*)	R/L (*wt/wt*)	pH	ρ_b (g/cm^3)
CG0	0	0.316	0.511	0.170	0.0044	0	---	7.27	0.967
CG22	0.070	0.246	0.511	0.170	0.0044	22	3.55	6.51	0.595
CG27	0.086	0.230	0.511	0.170	0.0044	27	2.68	5.99	0.552

2.2. Physic-chemical and electrochemical characterization methods

All materials were characterized by N_2 and CO_2 adsorption at -196 °C and 0 ºC, respectively. Adsorption isotherms were measured with an Autosorb 1 from Quantachrome after outgassing samples overnight at 110 ºC under high vacuum (10^{-6} mbar). N_2 adsorption isotherms were analyzed by BET equation, from which the surface area, S_{BET}, was obtained. The Dubinin-Radushkevich (DR) equation was applied to N_2 and CO_2 adsorption isotherms at -196 and 0 ºC, respectively, yielding the micropore volume, W_0, and the characteristic adsorption energy, E_0. The mean micropore width is given by $L_0=24/E_0$, this equation is valid for E_0 values lower than 20 kJ/mol, which correspond to pore widths higher than 1.3 nm [15].

The volume of nitrogen adsorbed at a relative pressure of 0.95, $V_{0.95}$, was considered as the total pore volume measurable obtained from the N_2 adsorption isotherms. The mesopore volume, V_{meso}, was obtained from the difference between $V_{0.95}$ and $W_0(N_2)$ [16]. The pore size distributions (PSDs) were obtained from N_2 isotherms by application of density functional theory (DFT) model [17], considering slit–shaped pores.

Chemical and structural differences between raw lignin and activated carbon xerogels were analyzed by Total Attenuated Reflectance (ATR). All spectra were constructed at the region from 4000 to 400 cm^{-1} with a resolution of 4 cm^{-1} and 64 scans. For ATR was used a FTIR spectrometer (Nicolet 6700) equipped with an ATR crystal in type IIA diamond mounted on tungsten carbide. Diamond ATR has a sampling area of approximately 0.5 mm^2, which applies a constant pressure to each sample. The weight loss behavior of the samples was measured using a thermobalance Mettler Toledo TGA/SDTA 851 E. Samples were heated to 1000 °C at a heating rate of 10 °C/min under N_2 flow.

The activated carbon xerogels were analyzed by scanning electron microscopy (SEM) by using a microscope Jeol JSM 5910 LV operated at 10 KV equipped with backscattered and secondary electron detectors coupled with Energy Dispersive Spectrometry (EDS). Surface acid groups on activated carbons were determinated by titration with NaOH [18].

Electrochemical measurements were carried out in a multichannel potentiostat Biologic VMP at room temperature using 1 M H_2SO_4 as electrolyte using a typical three- and two-cell configuration. The working electrodes were prepared by using a graphite paper pasted with a homogeneous mixture of the finely ground activated carbon xerogeles, acetylene black, and binder (polytetrafluoroethylene, PTFE) at mass ratio of 80:10:10. Cyclic voltammetry (CV), Chronopotentiometry (CP) and Electrochemical Impedance Spectroscopy (EIS) techniques were applied to estimate the presence or lack of pseudocapacitance effects of the carbon electrode materials [19] and gravimetric capacitance value. The gravimetric capacitance, C_{CP} (F/g), was

obtained from chronopotentiometry measurements by $C_{CP}=I_d\,\Delta t/(m\Delta V)$, where I_d is the discharge current (A), Δt is the discharge time (s), m is the mass electrode (g), and ΔV is the potential interval (V).

3. Results and discussion

Fig.1(a) depicts the N_2 adsorption-desorption isotherms on the activated carbon xerogels, which belong to type I of the IUPAC classification [20], typical of microporous solids. The isotherms show no hysteresis loop over the entire relative pressure range, indicating the absence of mesopores wider than 4 nm. However, there is also some mesoporosity, because the N_2 uptake slightly increases at higher relative pressure after micropore filling. The pore-size distributions (PSDs) are similar distribution for the activated carbon xerogels CG0A and CG22A, and a small increase of microporous volume accumulated for sample CG27A.

Table 2 compiles the surface area and porosity values obtained from the adsorption isotherms of CO_2 at 0 ºC and N_2 at -196 ºC. $W_0(N_2) > W_0(CO_2)$ in all samples, which suggests a high degree of activation and a heterogeneous size distribution of the micropores. In this case the N_2 is able to fill the total volume of micropores, obtained from adsorption at -196 °C. The CO_2 at 0 °C only fills the narrowest micropores (less than 0.7-0.8 nm wide) or ultramicropores [21]. Sample CG27A showed the highest S_{BET} (1243 m^2/g) and microporosity, these values slightly higher than showed by Hayashi et al. for activated carbon from lignin by chemical activation with H_3PO_4 at 1/1 impregnation ratio [22]. This behavior could be associated with pH of the initial dissolution that controls the kinetic polymerization and crosslinking, therefore, the morphology, particle size and porosity of the final gels [23]. At high pH, the polymerization-condensation is more difficult; addition reaction is promoted and methylol derivatives that form small clusters are created and the structures resulted would have a less porous development [24]. The sample CG27A showed the lowest pH of initial dissolution and bulk density of dried organic xerogels.

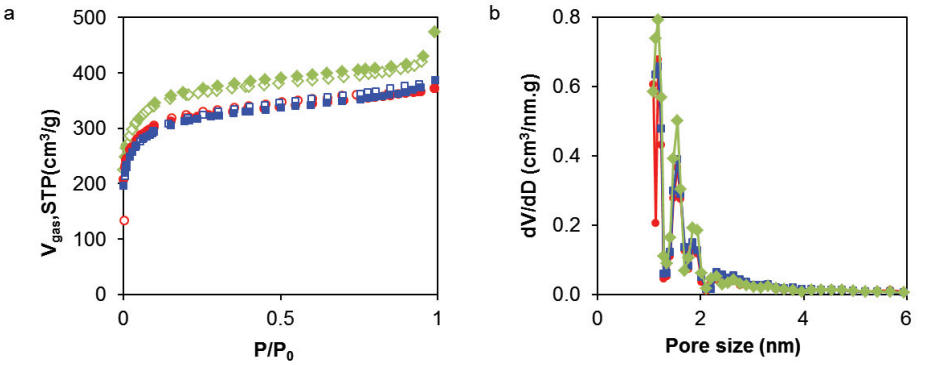

Fig. 1. (a) N_2 adsorption–desorption isotherms at -196 ºC; (b) The pore-size distributions by application of the DFT method of the samples CG0A (●-○), CG22A (■-□) and CG27A (♦-◊).

Table 2. Porosity and surface area of activated carbon xerogels.

Sample	S_{BET} (m^2/g)	$W_0(N_2)$ (cm^3/g)	$W_0(CO_2)$ (cm^3/g)	$V_{0.95}$ (cm^3/g)	V_{meso} (cm^3/g)	$L_0(N_2)$ (nm)	$L_0(CO_2)$ (nm)
CG0A	1101	0.455	0.290	0.519	0.065	1.43	0.63
CG22A	1069	0.443	0.247	0.529	0.086	1.50	0.72
CG27A	1243	0.518	0.310	0.595	0.077	1.56	0.66

The surface morphology of raw lignin corresponds to a tri-dimensional polymer as showed in [14]. Sample CG0A (Fig. 2(a)) showed a continuous, compact and without voids carbonaceous structure. On the other hand, samples CG22A (Fig. 2(b)) and CG27A (Fig. 2(c)) showed morphologies with large voids due to the high interaction between the chemical agent and lignin. Lignin has less reactive sites per mass than resorcinol and it is cross-linked with resorcinol and formaldehyde by addition and condensation reactions through a number of different ether (C-O-C) and carbon-carbon (C-C) bonds that are randomly distributed [12,25,26]. Macropores on xerogels are induced due to the large size of lignin molecule, it does not allow a good packing and also prevents shrinkage [10,14,27].

Table 3. Chemical composition of activated carbon xerogels from EDS analysis and surface acid groups.

Sample	Carbon (*wt.%*)	Oxygen (*wt.%*)	Phosphorus (*wt.%*)	Acid groups (*mmol/g*)
CG0A	77.76	13.25	8.99	4.90
CG22A	73.71	23.52	2.76	3.99
CG27A	84.39	13.29	2.32	5.09

In Table 3 is showed the chemical composition from Energy Dispersive X-ray Spectroscopy (EDS) analysis and surface acids groups. The percentage of Phosphorus decreased as the substitution of lignin increased. Acid groups values are similar in CG0A and CG27A carbon xerogels; this is according with wider peak between 1600 and 1500 cm^{-1} from FT-IR spectra showed in Fig. 3.

Fig. 3 shows FT-IR spectra and TGA/DTA profiles for all samples. The IR spectrum (Fig. 3(a)) of the lignin showed bands: –OH vibration stretching of hydroxyl groups involved in hydrogen bonding possibly due to adsorbed water (3400 – 3600 cm^{-1}) [28], asymmetric stretching of CH_2 (2920 cm^{-1}), stretching of CH_2 from aromatic methoxy groups (2850 cm^{-1}), CO_2 band (around 2362 cm^{-1}) could correspond to CO_2 existing in air or part of the carbon material reacts with the residual oxygen in inert nitrogen [29], stretching of carbonyls and C=O from conjugated ketones (1670 to 1730 cm^{-1}), deformation (shearing) of CH_2 and CH_3 (1420 cm^{-1}), stretching of C–O in guaiacyl ring (1220 cm^{-1}) [12]. The IR bands between 1600 and 1500 cm^{-1} correspond to deformation of C=C in aromatic rings, 1460 cm^{-1} originated from asymmetric C–H deformation, and the IR bands between 1160 and 850 cm^{-1} correspond to asymmetric and symmetric stretching of C–O–C, and out-of-plane deformation of C–H in aromatic rings [30]. The adsorption band around 3400-3600 cm^{-1} decreased after the activated process with H_3PO_4. Small differences in band intensities could be detect, which indicate some small differences in the surface chemistry. The absorption band around 2920 cm^{-1} was slightly wider for CG0A > CG22A > CG27A, while the sample CG27A showed a wider peak between 1600 and 1500 cm^{-1} respect to CG0A and CG22A.

The TGA (Fig. 3(b)) profiles were similar for the three samples showing a four-stage variation. The first stage of weight loss was between 30 and 120 ºC, attributed to the evaporation of surface adsorbed water [31]. At the first stage, activated bio-xerogels samples presented less weight loss than a conventional activated carbon xerogel. At the second stage, between 160 and 600 ºC, activated bio-xerogels samples exhibited also less weight loss than CG0A.

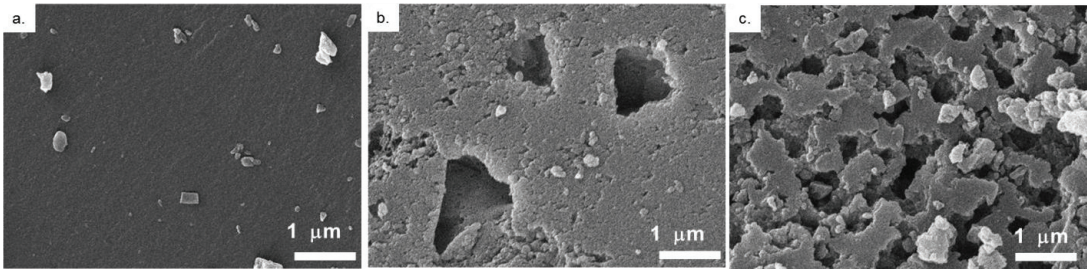

Fig. 2. SEM micrographs at 20 kV and X20000 of (a) activated carbon xerogel CG0A; (b) activated carbon bio-xerogel CG22A; (c) activated carbon bio-xerogel CG27A.

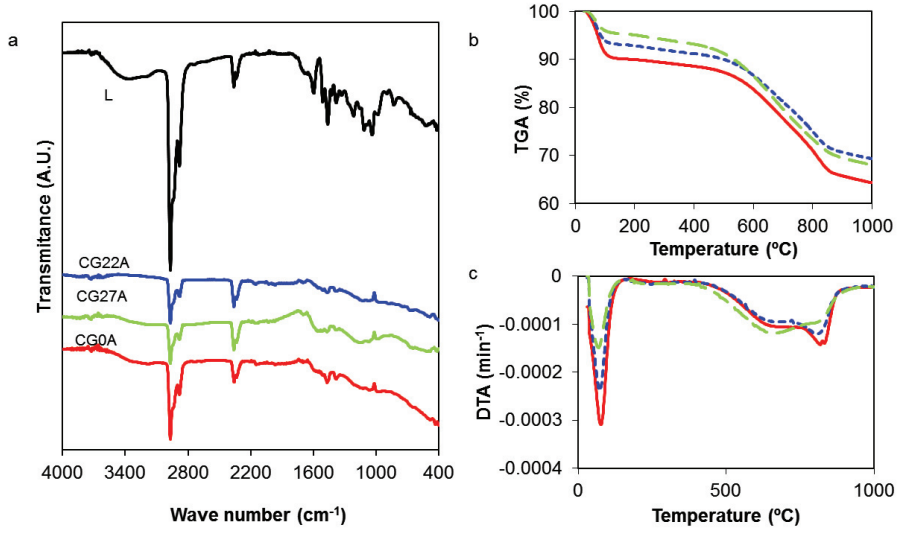

Fig. 3. (a) FT-IR spectra of raw lignin and, activated carbon xerogels; (b) Thermogravimetric analysis curves (TGA); (c) Differential thermal analysis curves (DTA) in samples CG0A (—), CG22A (– –) and CG27A (— —).

This stage corresponds to the decomposition and fragmentation of aromatic rings, C-O bindings and C-H bindings, a carbonization process due that activation was performed at 450 °C. The third mass loss, between 600 and 870 ºC, is due to a layer of phosphates and polyphosphates esters formed through activation with H_3PO_4, which could protect xerogels from excessive burn-off. At the third stage phosphate bridges break down occurs. Lignin addition reduces phosphorous incorporation, and reduces the total weight loss of about 65 % for CG0A and 68 % for CG22A and CG027A. The DTA profiles showed peaks at 75, 269, 660 and 820 ºC (Fig. 3(c)). In the temperature range of 250 to 750 ºC could be attributed to two different decomposition reactions involved in the carbonization process. One of these two decomposition reactions may correspond to breaking C-O bonds (200 – 300 kJ/mol) at the lower temperature and breaking C-H bonds (400 – 500 kJ/mol) at the higher temperature, according to bond strength data [24]. The CG27A sample has a wider peak between 400 and 750 ºC, which could be attributed to the impregnation of the H_3PO_4 as an activating agent with the lignin [22].

Fig. 4(a) shows the cyclic voltammograms (CVs) at 0.5 mV/g and Fig. 4(b) the chronopotentiograms (CPs) at 0.125 A/g for the three activated carbons xerogels in 1 M H_2SO_4. Sample CG0A showed non-rectangular and symmetric CVs, while samples CG22A and CG27A have a quasi-rectangular and symmetric shape profile and their CPs are triangular and symmetric, indicating that these two samples behave as an ideal Electric Double-Layer Capacitor (EDLC). CVs of activated carbon bio-xerogels showed small and wide humps at around 0.3 V, attributable to pseudo-faradaic reactions related to surface functionalities such as oxygen- and nitrogen-containing complexes [32].

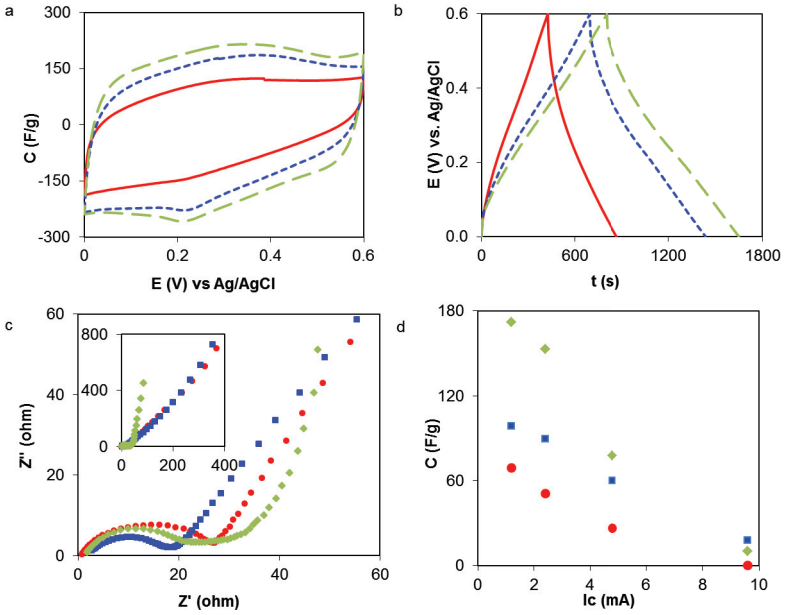

Fig. 4. (a) Cyclic voltammograms at 0.5 mV/s; (b) Chronopotentiograms at 0.125 A/g in samples CG0A (—), CG22A (– –) and CG27A (— —) using a three-electrode cell in 1 M H_2SO_4; (c) Impedance spectroscopy; (d) Variation of capacitance (C_{CP}) with current in samples CG0A (●), CG22A (■) and CG27A (♦) using a two-electrode cell in 1 M H_2SO_4.

The resistance of supercapacitors is obtained by impedance Nyquist plots (Fig. 4(c)). They show a semicircle in the high frequency region, which reflects the sum of the electrolyte resistance, R_s (Ω), and the resistance due to ion diffusion through the carbon pore network, R_p (Ω). R_s is obtained from the crossover point of the highest frequency (100 kHz) and the real part of the impedance and R_p is the diameter of the semicircle. The equivalent series resistance (ESR) is deduced from the intersect point of the impedance with the real axis in the low frequency region [19]. The diameter of the semicircle decreases in the order CG0A > CG27A > CG22A, which is associated with the diminution of the ESR. This behavior is attributable to a fast mass transport within the micropores and to the increase in oxygen content improving the wettability of the active material. Sample CG22A showed the highest percentage of oxygen as is showed in Table 3 (23.52 wt.%) [16]. At low frequencies, sample CG27A shows the best capacitive behavior (Fig. 4(c) inside) associated with a conductive performance and its microporous characteristics. As is showed in Fig. 4(d), the C_{CP} value decreases when current increases from 1.2 to 9.6 mA, because the formation of the EDLC within the micropores is less complete.

Table 4 shows the electrochemical characteristics at three- and two-cell configuration. The C_{CP} values are lower in two-cell configuration than three-, due to the two-cell configuration is closest to the real operation of a supercapacitor. Sample CG27A showed the highest C_{CP} value at both configurations using different techniques. Moreover, sample CG27A showed the highest BET surface area, volume and width micropores, and acid functional groups. In theory, the surface area has a directly

relationship with the energy storage capacitance [33], but this behavior must be accompanied by an appropriate size of micropores that allows the formation of the EDLC [19].

Chemical treatment of carbons significantly enriches the surface functionality often with enhancing the surface area, but in some cases the resistivity can be also increased as is seen in Fig. 4(c) and in the value of ESR. Moreover, the retention of capacity of sample CG27A at the highest current evaluated (9.6 mA) decreases significantly compared with sample CG22A. This behavior could be associated with the lower ESR presented and the higher presence of mesopores in sample CG22A respect to samples CG0A and CG27A. Mesopores connect the micropores and are necessary for a fast accessibility of the electrolyte ions into the micropores.

Table 4. Electrochemical characteristics of the activated carbon xerogels from three and two cell configurations.

Cell configuration	Three-	Two-				
Sample	C_{CP} (*F/g*)	Rs (*Ω*)	Rp (*Ω*)	ESR (*Ω*)	C_{CP} (*F/g*)	Retention (%)
	0.125 A/g	100 kHz			1.2 mA	9.6 mA
CG0A	139.8	1.0	26.0	26.5	69.1	0
CG22A	216.3	2.0	18.4	19.0	59.5	18
CG27A	234.3	1.2	22.0	33.0	172.1	6

Recently, Abioye and Ani [13] presented a review about the production of activated carbon electrodes from agricultural waste biomass for application in supercapacitors. The value of the gravimetric capacity, reported by different researches, ranged between 69 and 374 F/g in H_2SO_4. In this review, it can be concluded that surface chemistry and surface functionalities on the surface of activated carbons impacted more on the electrochemical properties than the physicochemical properties.

4. Conclusions

Activated carbon bio-xerogels were obtained with a carbonaceous structure basically microporous. A surface area as high as 1243 m^2/g is obtained after H_3PO_4-activation of organic carbon xerogels with a mass fractions of 0.086 equivalent to 27 of mass ratio (CG027A).

All activated carbon xerogels showed $W_0(N_2) > W_0(CO_2)$, which suggests a high degree of activation and a heterogeneous size distribution of the micropores. An increase in the percentage of lignin showed a high presence of acid groups the total.

The gravimetric capacitance increases with total micropores volume increased, reaching the highest value of gravimetric capacitance at 0.125 A/g was 234.2 F/g (CG027A) in a three-cell configuration and 172.1 F/g at 1.2 mA in a two-cell configuration. Sample CG22A showed a better retention of capacity, at the highest current value, due to the presence of mesoporos on the carbonaceous structure and the lowest ESR.

The electrochemical performance of activated carbon bio-xerogels prepared by H_3PO_4-activation was compared with published reports on other activated carbons, demonstrating that lignin could be an excellent precursor and partial substitute of resorcinol for the preparation of porous activated carbons for supercapacitor applications.

Acknowledgements

This work is part of the project “Desarrollo de electrodos para supercondensadores a partir de xerogeles de carbono funcionalizados con lignina y triazina” and is financed by COLCIENCIAS 658-2014 (Code: 121065842324). CDC acknowledges to COLCIENCIAS 2011 and UPB for doctoral study grant and financial support (Code: 113B-05/13-21). AUIP financed the international internship of CDC at Grupo de Investigación de Materiales de Carbón, Universidad de Granada (España), where the electrochemical measurements were carried out.

References

[1] R. Pekala, Low density, resorcinol-formaldehyde aerogels, 1989.

[2] J. Chen, R. Wang, J. Zhang, F. He, S. Han, Effects of preparation methods on properties of Ni/CeO2–Al2O3 catalysts for methane reforming with carbon dioxide, J. Mol. Catal. A Chem. 235 (2005) 302–310.

[3] J.C. Calderón, N. Mahata, M.F.R. Pereira, J.L. Figueiredo, V.R. Fernandes, C.M. Rangel, et al., Pt–Ru catalysts supported on carbon xerogels for PEM fuel cells, Int. J. Hydrogen Energy. 37 (2012) 7200–7211.

[4] J. Feng, C. Zhang, J. Feng, Carbon fiber reinforced carbon aerogel composites for thermal insulation prepared by soft reinforcement, Mater. Lett. 67 (2012) 266–268.

[5] Y.J. Lee, J.C. Jung, J. Yi, S.H. Baeck, J.R. Yoon, I.K. Song, Preparation of carbon aerogel in ambient conditions for electrical double-layer capacitor, Curr. Appl. Phys. 10 (2010) 682–686.

[6] C. Moreno-Castilla, M.B. Dawidziuk, F. Carrasco-Marín, E. Morallón, Electrochemical performance of carbon gels with variable surface chemistry and physics, Carbon N. Y. 50 (2012) 3324–32.

[7] R. Petričević, M. Glora, J. Fricke, Planar fibre reinforced carbon aerogels for application in PEM fuel cells, Carbon N. Y. 39 (2001) 857–67.
[8] N. Rey-Raap, A. Szczurek, V. Fierro, J.A. Menéndez, A. Arenillas, A. Celzard, Towards a feasible and scalable production of bio-xerogels, J. Colloid Interface Sci. 456 (2015) 138–144.
[9] Suhas, P.J.. Carrott, M.M.L. Ribeiro Carrott, Lignin - from natural adsorbent to activated carbon: A review, Bioresour. Technol. 98 (2007) 2301–12.
[10] F. Chen, M. Xu, L. Wang, J. Li, Preparation and characterization of organic aerogels from a lignin - resorcinol - formaldehíde copolymer, Bioresources. 6 (2011) 1262–1272.
[11] V.K. Thakur, M.K. Thakur, Recent advances in green hydrogels from lignin: A review, Int. J. Biol. Macromol. 72 (2015) 834–847.
[12] L.I. Grishechko, G. Amaral-Labat, A. Szczurek, V. Fierro, B.N. Kuznetsov, A. Pizzi, et al., New tannin–lignin aerogels, Ind. Crops Prod. 41 (2013) 347–355.
[13] A.M. Abioye, F.N. Ani, F. Nasir, Recent development in the production of activated carbon electrodes from agricultural waste biomass for supercapacitors: A review, Renew. Sustain. Energy Rev. 52 (2015) 1282–1293.
[14] C.D. Castro, G.C. Quintana, Mixture Design Approach on the Physical Properties of Lignin-Resorcinol-Formaldehyde Xerogels, Int. J. Polym. Sci. 2015 (2015) 11.
[15] M. Dubinin, Generalization of the theory of volume filling of micropores to nonhomogeneous microporous structures, Carbon N. Y. 23 (1985) 373–80.
[16] Z. Zapata-Benabithe, F. Carrasco-Marín, C. Moreno-Castilla, Preparation, surface characteristics, and electrochemical double-layer capacitance of KOH-activated carbon aerogels and their O- and N-doped derivatives, J. Power Sources. 219 (2012) 80–8.
[17] P. Tarazona, Solid-fluid transition and interfaces with density functional approaches, Surf. Sci. 331-333 (1995) 989–994.
[18] H.P. Boehm, Some aspects of the surface chemistry of carbon blacks and other carbons, Carbon N. Y. 32 (1994) 759–769.
[19] E. Frackowiak, F. Béguin, Carbon materials for the electrochemical storage of energy in capacitors, Carbon N. Y. 39 (2001) 937–50.
[20] K. Sing, D. Everett, R. Haul, L. Moscou, R. Pierotti, J. Rouquerol, et al., Reporting physisorption data for gas/solid systems with Special Reference to the Determination of Surface Area and Porosity, Pure Appl. Chem. 57 (1985) 603–619.
[21] F. Rodríguez-Reinoso, A. Linares-Solano, Microporous Structure of Activated Carbons as Revealed by Adsorption Methods, in: P. Thrower (Ed.), Chem. Phys. Carbon, Marcel Dekker INC, New York, 1989: pp. 1–146.
[22] J. Hayashi, A. Kazehaya, K. Muroyama, A.P. Watkinson, Preparation of activated carbon from lignin by chemical activation, Carbon N. Y. 38 (2000) 1873–1878.
[23] D. Fairén-Jiménez, F. Carrasco-Marín, C. Moreno-Castilla, Inter- and intra-Primary-Particle Structure of Monolithic Carbon Aerogels Obtained with Varying Solvents, Langmuir. 24 (2008) 2820–5.
[24] C. Lin, J. Ritter, Effect of synthesis pH on the structure of carbon xerogels, Carbon N. Y. 35 (1997) 1271–8.
[25] L.I. Grishechko, G. Amaral-Labat, a. Szczurek, V. Fierro, B.N. Kuznetsov, a. Celzard, Lignin-phenol-formaldehyde aerogels and cryogels, Microporous Mesoporous Mater. 168 (2013) 19–29. doi:10.1016/j.micromeso.2012.09.024.
[26] M. V. Alonso, M. Oliet, J. García, F. Rodríguez, J. Echeverría, Gelation and isoconversional kinetic analysis of lignin-phenol-formaldehyde resol resins cure, Chem. Eng. J. 122 (2006) 159–166. doi:10.1016/j.cej.2006.06.008.
[27] F. Chen, J. Li, Synthesis and Structural Characteristics of Organic Aerogels with Different Content of Lignin, Adv. Mater. Res. 113-116 (2010) 1837–1840.
[28] K. Suresh Kumar Reddy, A. Al Shoaibi, C. Srinivasakannan, A comparison of microstructure and adsorption characteristics of activated carbons by CO2 and H3PO4 activation from date palm pits, Xinxing Tan Cailiao/New Carbon Mater. 27 (2012) 344–351.
[29] W.C. Li, A.H. Lu, S.C. Guo, Characterization of the microstructures of organic and carbon aerogels based upon mixed cresol-formaldehyde, Carbon N. Y. 39 (2001) 1989–1994.
[30] H.B. Hergert, Lignins, occurrence, formation and reactions, in: Infrared Spectra, John Wiley & Sons, Inc., New York, 1971: pp. 267–297.
[31] J. Xu, L. Chen, H. Qu, Y. Jiao, J. Xie, Preparation and characterization of activated carbon from reedy grass leaves by chemical activation with H3PO4, Appl. Surf. Sci. 320 (2014) 674–680.
[32] K. Kinoshita, Carbon, Electrochemical and Physicochemical Properties, Jhon Wiley & Sons, Inc., Canada, 1988.
[33] B. Conway, Electrochemical Supercapacitors Scientific Fundamentals and Technological Applications, Kluwer Academic, New York, 1996.